
Learning Networked Linear Dynamical Systems under Non-white Excitation from a Single Trajectory

Harish Doddi*

Department of Mechanical Engineering
University of Minnesota Twin Cities
Minneapolis, MN 55455
doddi003@umn.edu

Deepjyoti Deka*

Theoretical Division T-5
Los Alamos National Laboratory
Los Alamos, NM 87545
deepjyoti@lanl.gov

Saurav Talukdar

Google Inc.
Mountain View, CA 94043
taluk005@umn.edu

Murti Salapaka

Department of Electrical & Computer Engineering
University of Minnesota Twin Cities
Minneapolis, MN 55455
murtis@umn.edu *

Abstract

We consider a networked linear dynamical system with p agents/nodes. We study the problem of learning the underlying graph of interactions/dependencies from observations of the nodal trajectories over a time-interval T . We present a regularized non-casual consistent estimator for this problem and analyze its sample complexity over two regimes: (a) where the interval T consists of n i.i.d. observation windows of length T/n (restart and record), and (b) where T is one continuous observation window (consecutive). Using the theory of M -estimators, we show that the estimator recovers the underlying interactions, in either regime, in a time-interval that is logarithmic in the system size p . To the best of our knowledge, this is the first work to analyze the sample complexity of learning linear dynamical systems *driven by unobserved not-white wide-sense stationary (WSS) inputs*.

1 Introduction

A networked linear dynamical system (LDS) is a network of agents/nodes, each of whose state evolves over time (in discrete or continuous steps) as a *linear* function of an external excitation and the states of its neighboring nodes in the network. The framework of LDS has been used to model dynamics in systems biology [1, 2], financial markets [3], energy [4], transportation [5] and other critical networks [6, 7]. Learning the dependencies, or topology learning, in a networked LDS is crucial for inference of influence pathways and subsequent control for the corresponding networks. As such, strategies to recover the underlying network structure from nodal time-series in LDS have been researched and can be classified into two categories: active and passive. Active learning involves efficient manipulation or interventions of nodal dependencies and injecting exogenous inputs into the LDS to infer the edges in the network by identifying the resulting changes [8]. Passive methods, on the other hand, use historical or streaming time-series of nodal states to infer the underlying topology. Our work falls within the domain of passive structure estimation. Very few works discuss learning such systems but are limited to the asymptotic regime (infinite sample limit). Examples include [9, 10, 11].

*First two authors have equal contribution. The authors acknowledge support from the Center for Non-Linear Studies (CNLS) and the Information Science and Technology Institute (ISTI) at Los Alamos National Laboratory.

Prior Work: Tractable passive topology learning in networked LDS and Vector Auto-Regressive processes (VAR) has been shown using the framework of l_1 -regularized regression ([12, 13] and references therein), where the focus is on extending the results from the static Lasso or Graphical Lasso [14, 15, 16] to one with correlated samples, by showing that properties such Restricted strong convexity hold. A similar approach for continuous time stochastic differential equation has been studied in [17]. A graphical model for VAR processes, without performance guarantees, has been proposed in [18]. Least squared regression based identification of unstable dynamical systems using a single trajectory has been studied in [19, 20]. However to the best of our knowledge, all existing work with sample complexity analysis of the learning algorithm relies on the assumption that unobserved exogenous inputs to the system are i.i.d. or white Gaussian noise, or that the exogenous inputs are observed [21, 22]. On learning networked LDS with temporally correlated inputs (wide-sense stationary and cyclo-stationary) using state observations (not inputs), [11] presents a consistent algorithm using non-causal regression (Wiener filter) for exact recovery. Similarly, [23] recovers the underlying topology in networked LDS using the framework of directed mutual information. However, these works do not provide for guarantees in the finite sample regime, aside from numerical examples. The overarching goal of this work is thus to provide a structure learning algorithm for networked LDS driven by temporally-correlated inputs, with guarantees on its performance at finite samples. We present a *regularized Wiener filter estimator* for this problem and use the theory of M -estimators to determine the observation window necessary to guarantee correct topology estimation.

The rest of the paper is organized as follows. In Section 2, we describe the mathematical model of networked linear dynamical system and our consistent learning algorithm. The main results are presented in Theorems 2.2 and 2.4. Section 3 contains results on M -estimators used in the proof of our theorems, with sketches of proofs in Section 4. Section 5 contains simulation results, and Section 6 summarizes the paper and includes potential extensions and generalizations.

2 Main Results

Consider a graph $G = (V, E)$ of $p + 1$ nodes in set $V = \{1, \dots, p + 1\}$ and undirected edge set $E \subset V \times V$. We denote the set of two-hop neighbors in G by set E_M , where $E_M = \{(i, j) | (i, j) \in E \text{ or } \exists k, \text{ s.t. } (ik), (jk) \in E\}$. Note that $E_M \setminus E$ is the set of ‘strict’ two-hop neighbors in the graph G , that do not form edges in E . Each node $i \in V$ is associated with a real-valued scalar state variable $\{x_i(k), k \in \mathbb{Z}\}$ that evolves in discrete time² according to the following linear dynamical equation:

$$x_i(k + 1) = h_{ii}x_i(k) + \sum_{(ij) \in E, j \neq i} h_{ij}x_j(k) + e_i(k), \quad (1)$$

where, $\{e_i(k), k \in \mathbb{Z}\}$, is an exogenous input. While samples of $x_i(k)$ are correlated in time due to the system dynamics, prior work on guaranteed learning of networked LDS include only temporally uncorrelated or white excitations/inputs $e_i(k)$. In this work, we consider $e(k)_{k \in \mathbb{Z}} = [e_1(k) \dots e_{p+1}(k)]^T$ to be a zero-mean **Wide-Sense Stationary (WSS)** Gaussian process, uncorrelated across nodes, i.e., $\forall k_1, k_2, \tau \in \mathbb{Z}$,

$$\begin{aligned} \mathbb{E}[e(k_1)] &= \mathbb{E}[e(k_2)] = 0, \text{ and} \\ \mathbb{E}[e(k_1 + \tau)e(k_1)^T] &= \mathbb{E}[e(k_2 + \tau)e(k_2)^T] \text{ is a diagonal matrix.} \end{aligned} \quad (2)$$

The time series vector $x(k)_{k \in \mathbb{Z}} = [x_1(k) \dots x_{p+1}(k)]^T \in \mathbb{R}^{p+1}$ is thus a zero mean jointly Gaussian WSS processes. We can write the frequency-domain representation of Eq. 1 at frequency $f \in [0, 2\pi)$ as,

$$X_i(f) = \sum_{(ij) \in E, j \neq i} H_{ij}(f)X_j(f) + P_i(f), \quad (3)$$

where, $H_{ij}(f) := [\mathcal{Z}[h_{ij}](z - \mathcal{Z}[h_{ii}])^{-1}]|_{z=e^{jf}}$ for $(ij) \in E$, is a linear time-invariant filter and $P_i(f) = [\mathcal{Z}[e_i](z - \mathcal{Z}[h_{ii}])^{-1}]|_{z=e^{jf}}$. Note that each edge $(ij) \in E$ corresponds to non-zero transfer functions H_{ij} and H_{ji} , that may be different. Given time-series of $\{x(k)\}$, we define the lagged correlation matrix $R_x(\tau)$ for $\tau \in \mathbb{Z}$, and its Discrete Time Fourier Transform (DTFT), namely, power

²we discuss extension to continuous time and higher order models in Section 6

spectral density Φ_x , at frequency f as

$$R_x(\tau) = \mathbb{E}(x(\tau)x^T(0)), \quad \Phi_x = \mathcal{F}\{R_x(\tau)\} = \lim_{m \rightarrow \infty} \sum_{p=-m}^m R_x(p)e^{-\iota fp}. \quad (4)$$

Topology Learning: Consider n state trajectories of all the nodes in V for the graph $G = (V, E)$ excited by *unobserved* WSS (temporally correlated) inputs, such that the r^{th} state trajectory (x^r) has N samples. Let $T = n \times N$ be equal to the total observation window. For the r^{th} state trajectory, define the Discrete Fourier Transform (DFT)³ is

$$X_i^r = \frac{1}{\sqrt{N}} \sum_{k=0}^{N-1} x_i^r(k)e^{-\iota fk}, \quad X_{\bar{i}}^r = \frac{1}{\sqrt{N}} \sum_{k=0}^{N-1} x_{\bar{i}}^r(k)e^{-\iota fk}, \quad (5)$$

where, $r \in \{1, \dots, n\}$, $x_{\bar{i}}^r = [x_1^r, \dots, x_{i-1}^r, x_{i+1}^r, \dots, x_{p+1}^r]^T$. Construct $\mathcal{Y} = [X_i^1, \dots, X_i^n]^T \in \mathbb{C}^n$ and $\mathcal{X} = [X_{\bar{i}}^1, \dots, X_{\bar{i}}^n]^T \in \mathbb{C}^{n \times p}$ respectively. We assume that \mathcal{X} and \mathcal{Y} are column-normalized, that is,

$$\frac{\|\mathcal{Y}\|_2}{\sqrt{n}} \leq 1, \quad \frac{\|\mathcal{X}(*, l)\|_2}{\sqrt{n}} \leq 1, \quad \forall l \in \{1, \dots, p\}. \quad (6)$$

For any quantity $\beta \in \mathbb{C}$, we use $\Re(\beta)$ and $\Im(\beta)$ to denote its real and imaginary components. We list the following result from [11] that enables consistent estimation of all edges in E (as described in Figure 1), using nodal state trajectories.

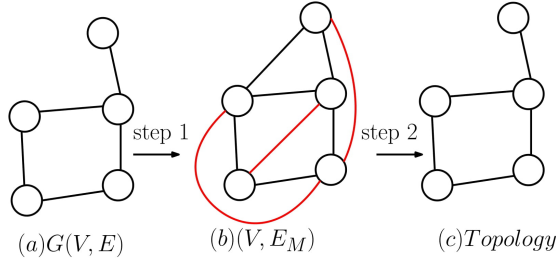


Figure 1: Topology Learning: In step 1, the two-hop neighborhood set E_M is estimated using Lemma 2.1(a). In step 2, strict two-hop neighbors (red colored edges) are eliminated from E_M using Lemma 2.1(b).

Lemma 2.1 ([11]). *For $i \in V$ of a well-posed networked LDS, the Wiener filter W_i in Eq. 7 satisfies (a) $W_i[j] \neq 0$ if and only if $(ij) \in E_M$ (b) for $(ij) \in E_M$, $\Im(W_i[j]) \neq 0$ if and only if (ij) is a true edge in G .*

$$W_i = \lim_{n, N \rightarrow \infty} \arg \min_{\beta \in \mathbb{C}^p} \frac{1}{2n} \|\mathcal{Y} - \mathcal{X}\beta\|_2^2, \quad (7)$$

The proof of Lemma 2.1 (see [11] for details) follows by showing that $W_i[j] = -[\Phi_x^{-1}(i, i)]^{-1} \Phi_x^{-1}(i, j)$. The result then follows from algebraic properties of Φ_x^{-1} (inverse power spectral density) derived from Eq. 3. It is worth noting that, in the time-domain, Eq. 7 is equivalent to a *non-causal* regression of the time-series, termed as “Wiener filter” [9]. This is effectively a *non-causal extension* of the connection between the inverse covariance matrix and the neighborhood regression used in learning static Gaussian graphical models [15, 16, 24]. For the finite sample regime, we study the problem of estimating edges \hat{E} such that $\mathbb{P}[\hat{E} = E] \geq 1 - \epsilon$ for any user-defined threshold $\epsilon \in (0, .5)$. Estimating Φ_x and then inverting it requires significant amount of data in the high dimensional setting. Instead, we use a regularized version of Eq. 7 as our graph estimator.

2.1 Regularized Wiener Filter Estimator

We propose a Regularized Wiener Filter Estimator \hat{W}_i for a node $i \in V$ as follows:

$$\hat{W}_i(\lambda) = \arg \min_{\beta \in \mathbb{C}^p} \frac{1}{2n} \|\mathcal{Y} - \mathcal{X}\beta\|_2^2 + \lambda \|\beta\|_1, \quad (8)$$

³computed at a fixed frequency $f = 2k\pi/N$, $k \in \{0, 1, \dots, N-1\}$ unless explicitly mentioned

where, $\lambda > 0$ is the regularization parameter. As $\beta \in \mathbb{C}^p$, $\|\beta\|_1$ is equal to the 1, 2-group norm over $[\Re(\beta) \Im(\beta)]$. For thresholds τ_1, τ_2 , we construct sets

$$\hat{E}_M := \{(ij) | |\hat{W}_i[j]| + |\hat{W}_j[i]| \geq \tau_1\}, \hat{E} := \{(ij) | (ij) \in \hat{E}_M, |\Im(\hat{W}_i[j])| + |\Im(\hat{W}_j[i])| \geq \tau_2\}. \quad (9)$$

In the remaining of the paper, we find sufficient conditions on n , N and λ and fix thresholds such that $\mathbb{P}[\hat{E} = E] \geq 1 - \epsilon$, for given $\epsilon \in (0, 0.5)$. We consider two settings: (i) **Restart & Record**: The n trajectories of length N each are independent, i.e., the system is reset or sufficient gap is provided before the next N time-intervals are recorded. Thus, $\{x^r\}_{r=1}^N$ are i.i.d., and (ii) **Consecutive**: In the second and more realistic setting, we consider the n state trajectories to be consecutive, i.e., $\{x^r\}_{r=1}^N$ correspond to N -length intervals from a larger trajectory of length $n \times N$. See Figure. 2 for the two settings considered in this article.

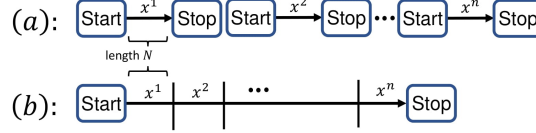


Figure 2: (a) i.i.d trajectories are generated using restart & record (b) a single trajectory is generated for the non i.i.d, consecutive setting.

2.2 Main Results

The error in estimating W_i by Eq. 8 and consequently in topology learning arises due to the finite N in computing \mathcal{X} by DFT, as well as the finite n in the empirical regression. For our analysis, we consider the following non-zero parameters of the LDS over graph $G = (V, E)$.

$$L = \lambda_{\min}(\Phi_x^{-1}); U = \lambda_{\max}(\Phi_x^{-1}); d = \max_{i \in V} \deg_{E_M}(i); \quad (10)$$

$$C > 0, \delta > 1, \text{ s.t. } \|R_x(\tau)\|_2 \leq C\delta^{-|\tau|}, \tau \in \mathbb{Z}; m_i = \min_{j | (ij) \in E} |\Im(W_i[j])|, m = \arg \min_{i \in V} m_i.$$

Note that under persistently exciting inputs, Φ_e is a positive definite matrix almost surely at all frequencies [9]. Further, G is a connected network. Hence, under standard well-posedness assumptions, $(\mathbb{I} - H)$ and P^{-1} in Eq. 3 in the main document are full-ranked and $L \geq 0$. Using norm bounds for matrix products, L and U can be bounded in terms of maximum and minimum eigen-values of $(\mathbb{I} - H^*)(\mathbb{I} - H)$ and P^{-1} . C, δ relate to the rate of decay of temporal correlation in the system states. Higher values of C and δ^{-1} imply greater temporal correlation. d , the maximum degree due to edges in E_M , is upper-bounded by the square of the maximum nodal degree in $G = (V, E)$.

For the case where the trajectories are i.i.d., the following theorem bounds the error in estimating W_i .

Theorem 2.1 (restart & record- squared error). Suppose $\epsilon_1 > 0$, $i \in V$, $4\sqrt{\frac{3 \log(8p/\epsilon_1)}{nL}} \leq \lambda \leq \frac{m_i}{1536U\sqrt{d}}$, $n \geq \max\{\frac{1}{c} \log \frac{4c'}{\epsilon_1}, (3456)^2(\frac{U}{L} + 0.5) \log(2p)d, 3(6144)^2 \frac{U^2}{L} d \log(\frac{8p}{\epsilon_1})(\frac{1}{m_i})^2\}$ and $N \geq \frac{4CU\delta^{-1}}{(1-\delta^{-1})^2}$, then $\|\hat{W}_i(\lambda) - W_i\|_2 \leq \frac{m_i}{2}$ holds with a probability of at least $1 - \epsilon_1$, where c, c' are universal positive constants. U, L, C, δ, m_i, d are defined in Eq. 10.

Using the above result, we prove our first result on the correctness of our thresholding procedure listed in Eq. 9 for i.i.d. trajectories. We recall that n is the number of realizations of time-series, each of length N .

Theorem 2.2 (restart & record- structure learning). Suppose $\epsilon > 0$. For $4\sqrt{\frac{3 \log(8p^2/\epsilon)}{nL}} \leq \lambda \leq \frac{m}{1536U\sqrt{d}}$, $n \geq \max\{\frac{1}{c} \log \frac{4c'p}{\epsilon}, (3456)^2(\frac{U}{L} + 0.5) \log(2p)d, 3(6144)^2 \frac{U^2}{L} d \log \frac{8p^2}{\epsilon} \frac{1}{m^2}\}$ for universal positive constants c, c' and $N \geq \frac{4CU\delta^{-1}}{(1-\delta^{-1})^2}$, construct an undirected edge set \hat{E}_M and \hat{E} as per Eq. 9 with thresholds $\tau_1 = \tau_2 = m$, then $E = \hat{E}$ holds with a probability of at least $1 - \epsilon$. U, L, C, δ, m, d are defined in Eq. 10.

The proofs of Theorems 2.1 and 2.2 are provided in Section 4. Next we consider the case where the n trajectories correspond to consecutive intervals from the same time-series of length $T = n \times N$. The following holds for the error for the regularized estimator in Eq. 8.

Theorem 2.3 (consecutive- squared error). Suppose $\epsilon_1 > 0$ such that $p \geq \sqrt{\frac{8}{\epsilon_1}}$ and $i \in V$. For $4\sqrt{\frac{(3+24\sqrt{3}UC(\delta-1)^{-1})\log(8p/\epsilon_1)}{nL}} \leq \lambda \leq \frac{m_i}{1536U\sqrt{d}}$, $n \geq \max\{33^2 \log p[\frac{U}{L} + 0.5 + 4\sqrt{8\frac{CU}{\delta-1}}]^2, 2\log(\frac{8p^2}{p^2\epsilon_1-8}), (3 + 24\sqrt{3}UC(\delta-1)^{-1})(6144)^2\frac{U^2}{L}d\log(\frac{8p}{\epsilon_1})(\frac{1}{m_i})^2\}$, and $N \geq \frac{4CU\delta^{-1}}{(1-\delta^{-1})^2}$, then we have $\|\hat{W}_i(\lambda) - W_i\|_2 \leq \frac{m_i}{2}$ holds with a probability of at least $1 - \epsilon_1$, where c, c' are universal positive constants. U, L, C, δ, m_i, d are defined in Eq. 10.

This leads to our second result on correct topology recovery in the non-i.i.d. case.

Theorem 2.4 (consecutive- structure learning). Suppose $\epsilon > 0$ such that $p \geq \frac{8}{\epsilon}$. Let $4\sqrt{\frac{(3+24\sqrt{3}UC(\delta-1)^{-1})\log(8p^2/\epsilon)}{nL}} \leq \lambda \leq \frac{m}{1536U\sqrt{d}}$, $n \geq \max\{33^2 \log p[\frac{U}{L} + 0.5 + 4\sqrt{8\frac{CU}{\delta-1}}]^2, 2\log(\frac{8p^2}{p^2\epsilon-8}), (3 + 24\sqrt{3}UC(\delta-1)^{-1})(6144)^2\frac{U^2}{L}d\log(\frac{8p^2}{\epsilon})\frac{1}{m^2}\}$ for a universal positive constants c, c' and $N \geq \frac{4CU\delta^{-1}}{(1-\delta^{-1})^2}$, construct an undirected edge set \hat{E}_M and \hat{E} as per Eq. 9 with thresholds $\tau_1 = \tau_2 = m$, then $E = \hat{E}$ holds with a probability of at least $1 - \epsilon$. U, L, C, δ, m, d are defined in Eq. 10.

The proof of Theorems 2.3 and 2.4 are provided in Section 4. In the next section, we present our approach for proving these theorems based on the theory of M-estimators [25], albeit in the complex domain.

3 Analysis of Regularized Wiener Filter Estimator

Our regularized regression involves working with complex-valued random variables $X_i^r, X_{\bar{i}}^r$ defined in Eq. 5 for a node $i \in V$. Their probability distribution is as follows,

$$\begin{bmatrix} X_i^r \\ X_{\bar{i}}^r \end{bmatrix} \sim \mathcal{N}(\mathbf{0}, \hat{\Phi}_x), \text{ where, } \hat{\Phi}_x = \begin{bmatrix} \hat{\Phi}_i & \hat{\Phi}_{i,\bar{i}} \\ \hat{\Phi}_{\bar{i},i} & \hat{\Phi}_{\bar{i}} \end{bmatrix} = \frac{1}{N} \sum_{q=-(N-1)}^{(N-1)} (N - |q|) R_x(q) e^{-\iota f q}. \quad (11)$$

Thus, $X_i^r \sim \mathcal{N}(0, \hat{\Phi}_i)$ and $X_{\bar{i}}^r \sim \mathcal{N}(\mathbf{0}, \hat{\Phi}_{\bar{i}})$. The following result bounds the difference between $\hat{\Phi}_x$ and Φ_x (see Eq. 4) for a N -length trajectory, and is used in our analysis.

Lemma 3.1. If $N > \frac{4CU\delta^{-1}}{(1-\delta^{-1})^2}$, then $\|\Phi_x - \hat{\Phi}_x\|_2 \leq \frac{1}{2U}$. Moreover, $\|\Phi_{\bar{i}} - \hat{\Phi}_{\bar{i}}\|_2 \leq \frac{1}{2U}$.

The proof is provided in the Appendix. The regularized Wiener filter estimator Eq. 8 belongs to a class of regularized M -estimators. Note that the regularizer $(\|\cdot\|_1)$ in Eq. 8 satisfies decomposability property with respect to the following complex-valued subspaces: $\mathcal{M} = \{v \in \mathbb{C}^p | v[j] = 0 \text{ if } W_i[j] = 0\}$, $\mathcal{M}^\perp = \{v \in \mathbb{C}^p | v[j] = 0 \text{ if } W_i[j] \neq 0\}$ for a node $i \in V$. That is, $\|v\|_1 = \|v_{\mathcal{M}}\|_1 + \|v_{\mathcal{M}^\perp}\|_1$, where $v_{\mathcal{M}}, v_{\mathcal{M}^\perp}$ are the projections of v on \mathcal{M} and \mathcal{M}^\perp . We follow the approach in [25] to bound the error

$$\hat{\Delta} := \hat{W}_i(\lambda) - W_i. \quad (12)$$

[25] states that only two conditions are sufficient to control the error $\|\hat{\Delta}\|_2$.

$$\text{First condition (choice of } \lambda): \lambda \geq \frac{2}{n} \|\mathcal{X}^H(\mathcal{Y} - \mathcal{X}W_i)\|_\infty. \quad (13)$$

As shown in [25], Eq. 13 ensures that $\hat{\Delta}$, defined in Eq. 12, belongs to the set

$$\mathcal{D}(W_i) = \{\Delta \in \mathbb{C}^p \mid \|\Delta_{\mathcal{M}^\perp}\|_1 \leq 3\|\Delta_{\mathcal{M}}\|_1\}. \quad (14)$$

$$\text{Second condition (restricted eigenvalue property): } \frac{1}{n} \|\mathcal{X}\Delta\|_2^2 \geq \kappa \|\Delta\|_2^2, \forall \Delta \in \mathcal{D}(W_i). \quad (15)$$

The following proposition, similar to Theorem 1 in [25], bounds the error $\|\hat{\Delta}\|_2$.

Proposition 1. For the regularized Wiener filter estimator defined in Eq. 8, $\|\hat{W}_i - W_i\|_2 \leq (\frac{3}{\kappa} \lambda \sqrt{d})$, whenever Eq. 13 and Eq. 15 hold.

For completion, we outline a proof of Eq. 14 and Proposition 1 for complex-valued variables in Appendix 7.2, following the real-valued analysis in [25]. We now show that Eq. 13 and Eq. 15 hold, for both *restart & record* (i.i.d.) and *consecutive* (non-i.i.d.) trajectories. These are then used to prove Theorems 2.2 and 2.4.

restart & record (i.i.d.) trajectories:

Lemma 3.2. Suppose $\epsilon_3 > 0$. Let rows in $\{X_i^r\}_{r=1}^n$ and $\{X_i^r\}_{r=1}^n$ defined in Eq. 5 be i.i.d. If $\lambda \geq 4\sqrt{\frac{3\log(4p/\epsilon_3)}{nL}}$, then $\lambda \geq \frac{2}{n}\|\mathcal{X}^H(\mathcal{Y} - \mathcal{X}W_i)\|_\infty$ holds with a probability of at least $1 - \epsilon_3$.

Lemma 3.3. Suppose $\epsilon_2 > 0$ be given. Let rows in $\{X_i^r\}_{r=1}^n$ and $\{X_i^r\}_{r=1}^n$ defined in Eq. 5 be i.i.d. If $n \geq \max\{\frac{1}{c}\log\frac{2c'}{\epsilon_2}, (3456)^2(\frac{U}{L} + 0.5)\log(2p)d\}$, $N \geq \frac{4CU\delta^{-1}}{(1-\delta^{-1})^2}$, then Eq. 15 holds with $\kappa = \frac{1}{256U}$, with a probability of at least $1 - \epsilon_2$.

The proofs for Lemmas 3.2 and 3.3 are provided in Section 4.1.

Consecutive (non i.i.d.) trajectories: For the non i.i.d. scenario, the guarantee on lambda and restricted eigenvalue condition are stated next with proofs provided in Section 4.2.

Lemma 3.4. Suppose $\epsilon_3 > 0$. Assume that both $\{X_i^r\}_{r=1}^n$ and $\{X_i^r\}_{r=1}^n$ defined in Eq. 5 are non i.i.d. If $\lambda \geq 4\sqrt{\frac{(3+24\sqrt{3}UC(\delta-1)^{-1})\log(4p/\epsilon_3)}{nL}}$, then $\lambda \geq \frac{2}{n}\|\mathcal{X}^H(\mathcal{Y} - \mathcal{X}W_i)\|_\infty$ holds with a probability of at least $1 - \epsilon_3$.

Lemma 3.5. Suppose $\epsilon_2 > 0$ such that $p \geq \sqrt{\frac{4}{\epsilon_2}}$. Assume that both $\{X_i^r\}_{r=1}^n$ and $\{X_i^r\}_{r=1}^n$ defined in Eq. 5 are non i.i.d. Then, if $n \geq \max\{33^2\log p[\frac{U}{L} + 0.5 + 4\sqrt{8\frac{CU}{\delta-1}}]^2, 2\log(\frac{4p^2}{p^2\epsilon_2-4})\}$, $N \geq \frac{4CU\delta^{-1}}{(1-\delta^{-1})^2}$, then $\frac{1}{n}\|\mathcal{X}\Delta\|_2^2 \geq \kappa\|\Delta\|_2^2$, holds for all $\Delta \in \mathcal{D}(W_i)$ with $\kappa = \frac{1}{256U}$, with a probability of at least $1 - \epsilon_2$.

4 Proof of Main Theorems

Proof of Theorem 2.1. For $n \geq \max\{\frac{1}{c}\log\frac{4c'}{\epsilon_1}, (3456)^2(\frac{U}{L} + 0.5)\log(2p)d\}$ and $N \geq \frac{4CU\delta^{-1}}{(1-\delta^{-1})^2}$, we apply Lemma 3.3 with $\epsilon_2 = \frac{\epsilon_1}{2}$, then Eq. 15 holds with probability of at least $1 - \frac{\epsilon_1}{2}$. Here, $\kappa = \frac{1}{256U}$. With $\lambda \geq 4\sqrt{\frac{3\log(8p/\epsilon_1)}{nL}}$, apply Lemma 3.2 with $\epsilon_3 = \frac{\epsilon_1}{2}$, then Eq. 13 holds with probability of at least $1 - \frac{\epsilon_1}{2}$. It follows from Proposition 1 that, $\|\hat{W}_i - W_i\|_2 \leq (\frac{3}{\kappa}\lambda\sqrt{d}) = (768U\lambda\sqrt{d})$. Take $\lambda \leq \frac{m_i}{1536U\sqrt{d}}$. For $n \geq 3(6144)^2\frac{U^2}{L}d\log(\frac{8p}{\epsilon_1})(\frac{1}{m_i})^2$, $4\sqrt{\frac{3\log(8p/\epsilon_1)}{nL}}$ is smaller than $\frac{m_i}{1536U\sqrt{d}}$. Thus, $\|\hat{W}_i - W_i\|_2 \leq \frac{m_i}{2}$ holds with a probability of at least $1 - \epsilon_1$. \square

Proof of Theorem 2.2. Choose $\epsilon_1 = \frac{\epsilon}{p}$. It follows from definition of m , that $\frac{1}{m} \geq \frac{1}{m_i}$ for all $i \in V$. Now $n \geq \max\{\frac{1}{c}\log\frac{4c'p}{\epsilon}, (3456)^2(\frac{U}{L} + 0.5)\log(2p)d, 3(6144)^2\frac{U^2}{L^2}d(\log\frac{8p^2}{\epsilon})(\frac{1}{m})^2\}$ and $4\sqrt{\frac{3\log(8p^2/\epsilon)}{nL}} \leq \lambda \leq \frac{m}{1536U\sqrt{d}}$ would satisfy the conditions on n and λ specified in Theorem 2.1 for a $i \in V$. Therefore, $\|\hat{W}_i - W_i\|_2 \leq \frac{m}{2}$ holds with a probability of at least $1 - \frac{\epsilon}{p}$. Using a union bound for all the $p+1$ nodes, we have $\|\mathfrak{S}[\hat{W}_i - W_i]\|_2 \leq \|\hat{W}_i - W_i\|_2 \leq \frac{m}{2}$ holds for all $i \in V$ with a probability of at least $1 - \frac{\epsilon(p+1)}{p} \approx 1 - \epsilon$ for large p .

Note that if $(ij) \in E$, then $|\mathfrak{S}(W_i[j])| \geq m > 0$. Similarly, for $(ij) \in E \setminus E_M$, $\mathfrak{S}(W_i[j]) = 0$ and for $(ij) \notin E_M$, $W_i[j] = 0$. Expanding $\|\hat{W}_i - W_i\|_2$, it can thus be shown that \hat{E} derived from \hat{E}_M contains only the edges in E . \square

Proof of Theorem 2.3. Here, we combine the results of Lemma 3.5 with $\epsilon_2 = \frac{\epsilon_1}{2}$ and Lemma 3.4 with $\epsilon_3 = \frac{\epsilon_1}{2}$. The rest of the proof is analogous to proof of Theorem 2.1.

Proof of Theorem 2.4. Using Theorem 2.3 for every node $i \in V$ with $\epsilon_1 = \frac{\epsilon}{p}$, the proof is analogous to the proof of Theorem 2.2. \square

Next we prove the lemmas on λ and restricted eigenvalue property, introduced in Section 3, that are used in the Theorems' proofs.

4.1 Proofs of M -estimator conditions for (restart & record) trajectories

Proof of Lemma 3.2. Let $\mathcal{E} := \mathcal{Y} - \mathcal{X}W_i$. We show that $\frac{1}{n}\|\mathcal{X}^H\mathcal{E}\|_\infty$ is bounded with a high probability and choose λ greater than that bound. Separating $\mathcal{X} = \mathcal{X}_R + \iota\mathcal{X}_I$, $\mathcal{E} = \mathcal{E}_R + \iota\mathcal{E}_I$, into real and imaginary parts (specified by subscripts R and I respectively), we have

$$\frac{1}{n}\|\mathcal{X}^H\mathcal{E}\|_\infty \leq \frac{1}{n}\left\|\begin{pmatrix} \mathcal{X}_R^T & \mathcal{X}_I^T \end{pmatrix} \begin{pmatrix} \mathcal{E}_R \\ \mathcal{E}_I \end{pmatrix}\right\|_\infty + \frac{1}{n}\left\|\begin{pmatrix} -\mathcal{X}_I^T & \mathcal{X}_R^T \end{pmatrix} \begin{pmatrix} \mathcal{E}_R \\ \mathcal{E}_I \end{pmatrix}\right\|_\infty. \quad (16)$$

Let $\mathcal{E}_1 := [\mathcal{E}_R[1] \ \mathcal{E}_I[1] \ \dots \ \mathcal{E}_R[n] \ \mathcal{E}_I[n]]^T$ with covariance matrix \mathcal{C}_1 . Note that $\begin{pmatrix} \mathcal{E}_R \\ \mathcal{E}_I \end{pmatrix} = P\mathcal{E}_1$, for some symmetric permutation matrix P , such that its covariance matrix $\mathcal{C}_2 = P\mathcal{C}_1P$. Rewriting $\begin{pmatrix} \mathcal{E}_R \\ \mathcal{E}_I \end{pmatrix} = \mathcal{C}_2^{1/2} \begin{pmatrix} \mathcal{W}_R \\ \mathcal{W}_I \end{pmatrix}$ in Eq. 16, where $\begin{pmatrix} \mathcal{W}_R \\ \mathcal{W}_I \end{pmatrix} \sim \mathcal{N}(0, I)$, we have

$$\frac{1}{n}\|\mathcal{X}^H\mathcal{E}\|_\infty \leq \frac{1}{n}\left\|\begin{pmatrix} \mathcal{X}_R^T & \mathcal{X}_I^T \end{pmatrix} \mathcal{C}_2^{1/2} \begin{pmatrix} \mathcal{W}_R \\ \mathcal{W}_I \end{pmatrix}\right\|_\infty + \frac{1}{n}\left\|\begin{pmatrix} -\mathcal{X}_I^T & \mathcal{X}_R^T \end{pmatrix} \mathcal{C}_2^{1/2} \begin{pmatrix} \mathcal{W}_R \\ \mathcal{W}_I \end{pmatrix}\right\|_\infty. \quad (17)$$

To bound the right side of Eq. 17, we first show that either function is Lipschitz. Consider first $f(\mathcal{W}_R, \mathcal{W}_I) := \frac{1}{n} \left(\mathcal{X}_R^T(j, :) \ \mathcal{X}_I^T(j, :) \right) \mathcal{C}_2^{1/2} \begin{pmatrix} \mathcal{W}_R \\ \mathcal{W}_I \end{pmatrix}$. Then,

$$\begin{aligned} \|f(\mathcal{W}_R, \mathcal{W}_I) - f(\mathcal{W}'_R, \mathcal{W}'_I)\|_2 &\leq \frac{1}{n} \left\| \begin{pmatrix} \mathcal{X}_R^T(j, :) & \mathcal{X}_I^T(j, :) \end{pmatrix} \right\|_2 \|\mathcal{C}_2^{1/2}\|_2 \left\| \begin{pmatrix} \mathcal{W}_R - \mathcal{W}'_R \\ \mathcal{W}_I - \mathcal{W}'_I \end{pmatrix} \right\|_2, \\ &\leq \frac{1}{\sqrt{n}} \|P\|_2 \|\mathcal{C}_1^{1/2}\|_2 \left\| \begin{pmatrix} \mathcal{W}_R - \mathcal{W}'_R \\ \mathcal{W}_I - \mathcal{W}'_I \end{pmatrix} \right\|_2, (\cdot \text{ using Eq. 6}) \\ &= \frac{1}{\sqrt{n}} \sqrt{\|\mathcal{C}\|_2} \left\| \begin{pmatrix} \mathcal{W}_R - \mathcal{W}'_R \\ \mathcal{W}_I - \mathcal{W}'_I \end{pmatrix} \right\|_2 = \sqrt{\frac{3}{2nL}} \left\| \begin{pmatrix} \mathcal{W}_R - \mathcal{W}'_R \\ \mathcal{W}_I - \mathcal{W}'_I \end{pmatrix} \right\|_2 (\cdot \text{ Lemma 7.2 in the Appendix}). \end{aligned} \quad (18)$$

Thus, f is a Lipschitz function with Lipschitz constant $\sqrt{\frac{3}{2nL}}$. Using [26]'s result on concentration of Lipschitz functions, we have, for $t > 0$, $\mathbb{P}[\frac{1}{n} \left\| \begin{pmatrix} \mathcal{X}_R^T(j, :) & \mathcal{X}_I^T(j, :) \end{pmatrix} \right\|_2 \mathcal{C}_2^{1/2} \begin{pmatrix} \mathcal{W}_R \\ \mathcal{W}_I \end{pmatrix} \geq t] \leq 2 \exp(-\frac{t^2 n L}{3})$. Choosing $t = \sqrt{\frac{3 \log(\frac{4p}{\epsilon_3})}{nL}}$ and the union bound for all $j \in \{1, \dots, p\}$, we have $\mathbb{P}[\frac{1}{n} \left\| \begin{pmatrix} \mathcal{X}_R^T & \mathcal{X}_I^T \end{pmatrix} \mathcal{C}_2^{1/2} \begin{pmatrix} \mathcal{W}_R \\ \mathcal{W}_I \end{pmatrix} \right\|_\infty \geq \sqrt{\frac{3 \log(\frac{4p}{\epsilon_3})}{nL}}] \leq \frac{\epsilon_3}{2}$. Using a similar analysis, $\mathbb{P}[\frac{1}{n} \left\| \begin{pmatrix} -\mathcal{X}_I^T & \mathcal{X}_R^T \end{pmatrix} \mathcal{C}_2^{1/2} \begin{pmatrix} \mathcal{W}_R \\ \mathcal{W}_I \end{pmatrix} \right\|_\infty \geq \sqrt{\frac{3 \log(\frac{4p}{\epsilon_3})}{nL}}] \leq \frac{\epsilon_3}{2}$. Choose $\lambda \geq 4\sqrt{\frac{3 \log(4p/\epsilon_3)}{nL}}$. Using the Union bound on Eq. 17, we have $\mathbb{P}[\frac{1}{n}\|\mathcal{X}^H\mathcal{E}\|_\infty \geq \lambda/2] \leq \epsilon_3$. \square

Proof of Lemma 3.3. Note that $\mathcal{X} = [X_i^1, \dots, X_i^n]^T$, where X_i^r is computed from r^{th} trajectory, defined in Eq. 5. Separating into real and imaginary parts, we have:

$$\frac{\|\mathcal{X}\Delta\|_2^2}{n} = \frac{\|(\mathcal{X}_R + \iota\mathcal{X}_I)(\Delta_R + \iota\Delta_I)\|_2^2}{n} = \frac{\|\mathcal{X}_1 v\|_2^2}{n} + \frac{\|\mathcal{X}_2 v\|_2^2}{n}, \quad (19)$$

where $\mathcal{X}_1 := [\mathcal{X}_R - \mathcal{X}_I]$, $\mathcal{X}_2 := [\mathcal{X}_I \ \mathcal{X}_R]$ and $v = (\Delta_R^T \ \Delta_I^T)^T$. For simplicity, in this proof we drop the superscript r in X_i^r and X_i^T . Note that the rows of \mathcal{X}_1 and \mathcal{X}_2 are i.i.d. samples of the real random vectors, $[(X_i)_R^T - (X_i)_I^T]^T$ and $[(X_i)_I^T \ (X_i)_R^T]^T$, respectively. To show that $\frac{1}{n}\|\mathcal{X}\Delta\|_2^2 \geq \kappa\|\Delta\|_2^2$ holds for all $\Delta \in \mathcal{D}(W_i)$ with high probability, we prove the restricted eigenvalue property for group structured norms on both terms in Eq. 19. Let $\bar{\Sigma}$ be the covariance of random vector $[(X_i)_R^T \ (X_i)_I^T]^T$. Then,

$$\bar{\Sigma} = \begin{bmatrix} \bar{\Sigma}_{11} & \bar{\Sigma}_{12} \\ \bar{\Sigma}_{21} & \bar{\Sigma}_{22} \end{bmatrix} = \begin{bmatrix} \mathbb{E}[(X_i)_R(X_i)_R^T] & \mathbb{E}[(X_i)_R(X_i)_I^T] \\ \mathbb{E}[(X_i)_I(X_i)_R^T] & \mathbb{E}[(X_i)_I(X_i)_I^T] \end{bmatrix}. \quad (20)$$

Thus, $[(X_{\bar{i}})_R^T - (X_{\bar{i}})_I^T]^T$ and $[(X_{\bar{i}})_I^T (X_{\bar{i}})_R^T]^T$ have means $\mathbf{0}$ and covariance Σ_1 and Σ_2 , respectively, where,

$$\Sigma_1 = \begin{bmatrix} I & 0 \\ 0 & -I \end{bmatrix} \bar{\Sigma} \begin{bmatrix} I & 0 \\ 0 & -I \end{bmatrix} = \begin{bmatrix} \bar{\Sigma}_{11} & -\bar{\Sigma}_{12} \\ -\bar{\Sigma}_{21} & \bar{\Sigma}_{22} \end{bmatrix}, \quad \Sigma_2 = \begin{bmatrix} \bar{\Sigma}_{22} & \bar{\Sigma}_{21} \\ \bar{\Sigma}_{12} & \bar{\Sigma}_{11} \end{bmatrix}. \quad (21)$$

From Eq. 19, $\|\Delta\|_1 = \|v\|_{1,2} := \sum_{j=1}^p \|[v[j] \ v[p+j]]^T\|_2$. Consider the following definitions: $\mathcal{M}_2 := \{c \in \mathbb{R}^{2p} \mid c[i] = 0, c[p+i] = 0, \text{ if } (W_i)_R[i] = 0, (W_i)_I[i] = 0\}$, $\mathcal{M}_2^\perp := \{c \in \mathbb{R}^{2p} \mid c[i] = 0, c[p+i] = 0, \text{ if } (W_i)_R[i] \neq 0, (W_i)_I[i] \neq 0\}$ and $\mathcal{D}_2(W_i) := \{v \in \mathbb{R}^{2p} \mid \|v_{\mathcal{M}_2^\perp}\|_{1,2} \leq 3\|v_{\mathcal{M}_2}\|_{1,2}\}$.

Clearly, if $\Delta \in \mathcal{D}(W_i)$, defined in Eq. 14, then $v \in \mathcal{D}_2(W_i)$ and vice versa. For $v \in \mathcal{D}_2$, the group norm $\|v\|_{1,2} \leq 4\|v_{\mathcal{M}_2}\|_{1,2}$. Using Cauchy Schwartz inequality and the definition of bounded degree d , it follows that, $\|v_{\mathcal{M}_2}\|_{1,2} \leq \sqrt{d}\|v\|_2$. Thus, $\|v\|_{1,2} \leq 4\sqrt{d}\|v\|_2$. Below is a result, derived from Section 5 of [25] and [27] for Gaussian random matrices.

Lemma 4.1. *For any Gaussian random matrix $\mathbb{X} \in \mathbb{R}^{n \times 2p}$ with i.i.d. $\mathcal{N}(0, \Sigma)$ rows, then there are universal positive constants c, c' such that with probability at least $1 - c' \exp(-cn)$,*

$$\frac{\|\mathbb{X}v\|_2}{\sqrt{n}} \geq \frac{1}{4}\|\Sigma^{1/2}v\|_2 - \frac{27}{\sqrt{n}}\sqrt{2\log(2p)}\rho(\Sigma)\|v\|_{1,2}. \quad (22)$$

where, $w \sim \mathcal{N}(0, \Sigma)$, $\rho(\Sigma) := \max_{j \in \{1, \dots, p\}, i \in \{1, 2\}} [\mathbb{E}((w_{G_j}(i))^2)]^{1/2}$.

We use Eq. 22 with $\mathbb{X} = \mathcal{X}_1$ and \mathcal{X}_2 to obtain a lower bound on $\frac{\|\mathcal{X}_1(\Delta_R^T \Delta_I^T)^T\|_2}{\sqrt{n}}$ and $\frac{\|\mathcal{X}_2(\Delta_R^T \Delta_I^T)^T\|_2}{\sqrt{n}}$. Note that, for $\bar{\Sigma}, \Sigma_1$ and Σ_2 defined in Eqs. 20, 21, we have $\rho(\bar{\Sigma}) = \rho(\Sigma_1) = \rho(\Sigma_2) = \max_j [\bar{\Sigma}_{jj}]^{1/2}$. Using the inequality $\sqrt{a^2 + b^2} \leq a + b \leq \sqrt{2(a^2 + b^2)}$ for two non-negative numbers a, b in Eq. 19, we get that the following holds with a probability of $1 - 2c' \exp(-cn)$, where c, c' are universal positive constants:

$$\begin{aligned} \frac{\|\mathcal{X}\Delta\|_2}{\sqrt{n}} &\geq \frac{1}{\sqrt{2}} \left[\frac{\|\mathcal{X}_1(\Delta_R^T \Delta_I^T)^T\|_2}{\sqrt{n}} + \frac{\|\mathcal{X}_2(\Delta_R^T \Delta_I^T)^T\|_2}{\sqrt{n}} \right] \\ &\geq \frac{1}{\sqrt{2}} \left[\frac{1}{4}(\|\Sigma_1^{1/2}v\|_2 + \|\Sigma_2^{1/2}v\|_2) - \frac{54}{\sqrt{n}}\sqrt{2\log(2p)}\rho(\bar{\Sigma})\|v\|_{1,2} \right] \\ &\geq \frac{1}{\sqrt{2}} \left[\frac{1}{4}\sqrt{v^T(\Sigma_1 + \Sigma_2)v} - \frac{54}{\sqrt{n}}\sqrt{2\log(2p)}\rho(\bar{\Sigma})\|v\|_{1,2} \right] \\ &\geq \frac{1}{\sqrt{2}} \left[\frac{1}{4}\lambda_{\min}((\Sigma_1 + \Sigma_2)^{1/2}) - \frac{54}{\sqrt{n}}\sqrt{2\log(2p)}\rho(\bar{\Sigma})4\sqrt{d}\|v\|_2 \right], \end{aligned} \quad (23)$$

Using Eq. 21, the definition of $\hat{\Phi}_{\bar{i}} := \mathbb{E}(X_{\bar{i}}(X_{\bar{i}})^H)$, for $v := [\Delta_R^T, \Delta_I^T]^T$, it follows that,

$$\begin{aligned} v^T(\Sigma_1 + \Sigma_2)v &= \Delta^H \hat{\Phi}_{\bar{i}} \Delta \quad (\because \Sigma_1 + \Sigma_2 = \begin{bmatrix} (\hat{\Phi}_{\bar{i}})_R & (\hat{\Phi}_{\bar{i}})_I \\ -(\hat{\Phi}_{\bar{i}})_I & (\hat{\Phi}_{\bar{i}})_R \end{bmatrix}) \\ \Rightarrow \frac{1}{2U}\|\Delta\|_2^2 &\leq v^T(\Sigma_1 + \Sigma_2)v \leq \left[\frac{1}{L} + \frac{1}{2U}\right]\|\Delta\|_2^2 \quad (\because \text{using Lemma 3.1}) \end{aligned} \quad (24)$$

Thus, $\lambda_{\min}((\Sigma_1 + \Sigma_2)^{1/2}) \geq \frac{1}{\sqrt{2U}}$, and $\rho(\bar{\Sigma}) \leq \rho(\Sigma_1 + \Sigma_2) \leq \|(\Sigma_1 + \Sigma_2)^{1/2}\|_2 = \|(\hat{\Phi}_{\bar{i}})^{1/2}\|_2 \leq \sqrt{\frac{1}{L} + \frac{1}{2U}}$. Thus, Eq. 23 is, $\frac{\|\mathcal{X}\Delta\|_2}{\sqrt{n}} \geq \left[\frac{1}{8\sqrt{U}} - \frac{54}{\sqrt{n}}\sqrt{\log(2p)}\left(\sqrt{\frac{1}{L} + \frac{1}{2U}}\right)4\sqrt{d}\right]\|\Delta\|_2$. Choose $n \geq \max\{\frac{1}{c} \log \frac{2c'}{\epsilon_2}, (3456)^2(\frac{U}{L} + 0.5) \log(2p)d\}$, then $\frac{54}{\sqrt{n}}\sqrt{\log(2p)}\left(\sqrt{\frac{1}{L} + \frac{1}{2U}}\right)4\sqrt{d} \leq \frac{1}{16\sqrt{U}}$. Hence, $\frac{\|\mathcal{X}\Delta\|_2}{\sqrt{n}} \geq \frac{1}{16\sqrt{U}}\|\Delta\|_2$, and Eq. 15 with $\kappa = \frac{1}{256U}$ with a probability of at least $1 - \epsilon_2$. \square

4.2 Proofs of M -estimator conditions for consecutive trajectories

Proof of Lemma 3.4. The approach for the proof is identical to the proof of Lemma 3.2, with few changes. Define $\mathcal{E} := \mathcal{Y} - \mathcal{X}W_i$. Let \mathcal{C}_1 be the covariance matrix of the vector $\mathcal{E}_1 := [\mathcal{E}_R[1] \ \mathcal{E}_I[1] \ \dots \ \mathcal{E}_R[n] \ \mathcal{E}_I[n]]^T$. The trajectories aren't independent and \mathcal{C}_1 is no more block-diagonal here. An upper bound for $\|\mathcal{C}_1\|_2$ for this case is provided in Lemma 7.3 in the Appendix. Using that, the Lipschitz constant of $f(\mathcal{W}_R, \mathcal{W}_I)$ in Eq. 18 becomes $\sqrt{\frac{3+24\sqrt{3}UC(\delta-1)^{-1}}{2nL}}$. Following Lemma 3.2, $\lambda \geq 4\sqrt{\frac{(3+24\sqrt{3}UC(\delta-1)^{-1}) \log(4p/\epsilon_3)}{nL}}$ gives the result. \square

Proof of Lemma 3.5. Let $Z := \mathcal{X}\Delta \in \mathbb{C}^n$. Its real and imaginary components are $Z_R = [\mathcal{X}_R - \mathcal{X}_I]v$ and $Z_I = [\mathcal{X}_I \ \mathcal{X}_R]v$ where $v = [\Delta_R^T \ \Delta_I^T]^T$. We find the lower bounds on $\frac{1}{n}\|Z_R\|_2^2$, $\frac{1}{n}\|Z_I\|_2^2$ and then combine them to obtain a lower bound of $\frac{1}{n}\|Z\|_2^2$. Applying Lemma I.2 from the Supplementary material of [28] on Z_R and Z_I , we have, with individual probability atleast $1 - [2\exp(-\frac{n(t-\frac{2}{\sqrt{n}})^2}{2}) + 2\exp(-\frac{n}{2})]$ for all $t \geq \frac{2}{\sqrt{n}}$,

$$\frac{1}{n}\|Z_R\|_2^2 \geq \frac{1}{n}\text{Tr}[\mathbb{E}(Z_R Z_R^T)] - 4t\|\mathbb{E}(Z_R Z_R^T)\|_2, \quad \frac{1}{n}\|Z_I\|_2^2 \geq \frac{1}{n}\text{Tr}[\mathbb{E}(Z_I Z_I^T)] - 4t\|\mathbb{E}(Z_I Z_I^T)\|_2. \quad (25)$$

Note that the diagonal values of $\mathbb{E}(Z_R Z_R^T)$ are all equal to $v^T \Sigma_1 v$, and those of $\mathbb{E}(Z_I Z_I^T)$ are equal to $v^T \Sigma_2 v$ with Σ_1, Σ_2 defined in Eq. 21. Using this with Lemma 7.1 in the Appendix, we get,

$$\begin{aligned} \frac{1}{n}\|Z\|_2^2 &= \frac{1}{n}\|Z_R\|_2^2 + \frac{1}{n}\|Z_I\|_2^2 \geq v^T(\Sigma_1 + \Sigma_2)v - 8t\|\Delta\|_2^2 \left[\frac{1}{L} + \frac{1}{2U} + 4\sqrt{8} \frac{C}{\delta-1} \right] \\ &\geq \frac{1}{2U}\|\Delta\|_2^2 - 8t\|\Delta\|_2^2 \left[\frac{1}{L} + \frac{1}{2U} + 4\sqrt{8} \frac{C}{\delta-1} \right], \quad (\cdot \text{ Eq. 24}) \end{aligned} \quad (26)$$

holds with probability of atleast $1 - [4\exp(-\frac{n(t-\frac{2}{\sqrt{n}})^2}{2}) + 4\exp(-\frac{n}{2})]$ for $t \geq \frac{2}{\sqrt{n}}$. Choose $t = \sqrt{\frac{4\log p}{n}} (> \frac{2}{\sqrt{n}}$ for a large n). Then for $n \geq 33^2 \log p [\frac{U}{L} + 0.5 + 4\sqrt{8} \frac{CU}{\delta-1}]^2$, $\frac{1}{n}\|\mathcal{X}\Delta\|_2^2 \geq \frac{1}{256U}\|\Delta\|_2^2$ holds with probability at least $1 - [\frac{4}{p^2} + 4\exp(-\frac{n}{2})]$. Since $p \geq \sqrt{\frac{4}{\epsilon_2}}$, the statement holds whenever $n \geq 2\log(\frac{4p^2}{p^2\epsilon_2-4})$. \square

5 Numerical Results

We demonstrate the numerical implementation of recovering topology on a Desktop PC with Intel Xeon E5-1620 Processor (8x 3.7 GHz) and 32 GB RAM. We considered a two-dimensional square grid G with $p+1$ nodes and generate samples for Eq. 1 with exogenous input $e(k) = s_p 5[w(k) - 0.3w(k-1)]$, where $w(k)$, $w(k-1)$ are sampled from a standard Normal distribution, $s_p \in \mathbb{R}^{(p+1) \times (p+1)}$ is a diagonal matrix containing constants; $h \in \mathbb{R}^{(p+1) \times (p+1)}$ is a weighted adjacency matrix. The scaling s_p is chosen such that \mathcal{X} and \mathcal{Y} in the estimator are column-normalized.

We reconstruct the topology with a probability of at least $1 - \epsilon$, where $\epsilon = 0.05$. The numerical experiments are conducted in MATLAB R2020b.

For a choice of n , we generate n trajectories, either independently (restart & record) or taken as consecutive intervals of a larger trajectory (consecutive). Each trajectory is of length $N = \frac{4CU\delta^{-1}}{(1-\delta^{-1})^2}$, rounded to the nearest integer. From the trajectories, we compute the samples $\{X_i^r, X_i^r\}_{r=1}^n$ for all the nodes $i \in V$ at frequency $f = \frac{\pi}{2}$. The Regularized Wiener Filter Estimator is solved using CVXR [29], with $\lambda = 4\sqrt{\frac{3\log(8p^2/\epsilon)}{nL}}$ if trajectories are i.i.d., $\lambda = 4\sqrt{\frac{(3+24\sqrt{3}UC(\delta-1)^{-1})\log(8p^2/\epsilon)}{nL}}$ if trajectories are non-i.i.d.. After solving for \hat{W}_i , we construct $\hat{E} = \{(i, j) \mid |\Im(\hat{W}_i[j])| + |\Im(\hat{W}_j[i])| \geq m\}$ (m defined in Eq. 10). The relative error in reconstructing the topology is defined as the sum of false positive and false negatives. n_{min} is the minimum value of n such that relative error is zero for 45 out of 45 random trials. The values of n_{min} for various values of p and δ for the i.i.d. and non-i.i.d. cases are shown in Figure. 3. In Figure 3(b), the correlation strength δ^{-1} of the trajectories is high, and consequently N is large. For small δ^{-1} , the length of each trajectory can be reduced significantly for reconstructing the topology. For example, in Figure 3(c), N is much smaller. Further, n_{min} is of the order of $\approx 10^7$ rather than a more conservative estimate of $\approx 10^{16}$ as provided by the main theorems.

6 Extensions and Path Forward

In this article, we presented a regularized Wiener filter estimator to learn the structure of a discrete-time networked LDS. We analyzed the sample complexity of our estimator and showed that it linearly depends the logarithm of the number of nodes p in two cases, one where trajectories of nodal states are collected in independent observation windows of equal length, and another where the trajectories pertain to a single continuous observation window.

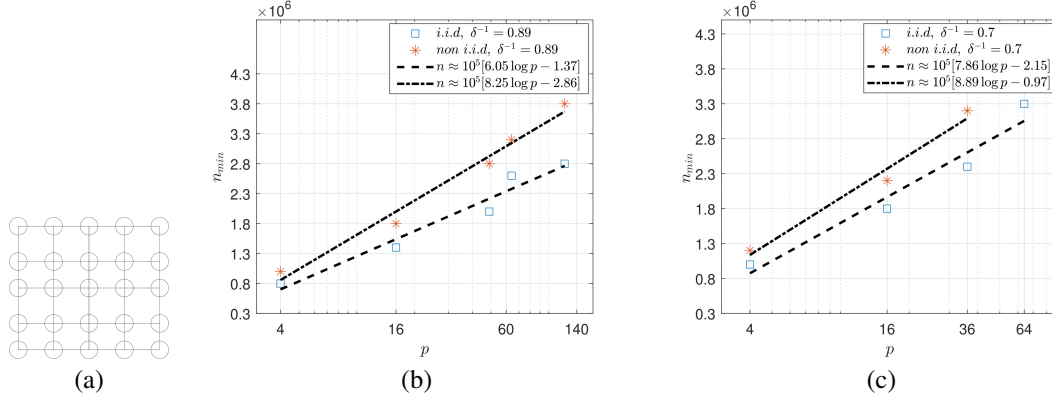


Figure 3: (a) An illustration of G as a 5×5 grid with $p = 24$. Dependence of n_{min} on $\log p$: (a) $C = 6.8$, $\delta^{-1} = 0.89$, $U = 1.55$, $L = 0.74$, $N = \frac{4CU\delta^{-1}}{(1-\delta^{-1})^2} \approx 2900$, (b) $C = 2.8$, $\delta^{-1} = 0.7$, $U = 1.3$, $L = 0.8$, $N = \frac{4CU\delta^{-1}}{(1-\delta^{-1})^2} \approx 115$.

While we discuss our method for first-order discrete-time LDS, our estimator can be extended to learning related networks as highlighted next.

VAR(p) models with correlated inputs: Lemma 2.1 and our subsequent analysis follows directly if higher-order delays (at the same node) are included in the LDS Eq. 1. L , U and the sample complexity will need to be changed accordingly.

Continuous time LDS: Considering a fixed sampling time ΔT and a time-discretization function, the continuous time LDS can be converted to a discrete-time LDS with related frequency domain-representation [11]. The analysis will involve merging the error due to discretization with the finite sample analysis.

LDS under cyclo-stationary processes: Cyclo-stationary processes represent a generalization of WSS processes where the statistics such as mean, correlation function are periodic functions of time. As shown in [30], a lifting operation can be used to represent time-evolution of a cyclo-stationary process as a WSS process with vector-valued states. The remaining analysis of the sample complexity will be similar but involve vector-valued states.

Directed graphs under correlated inputs: Note that our estimator uses properties of the inverse power spectral density (see Lemma 2.1 and discussion). Under a strict causality assumption on the linear filters [9, 23], it has been shown that directed edges can be recovered using inverse power spectral density. The framework presented here can thus be extended to efficiently learn the topology for strictly causal linear filters in the LDS setting.

Finally, we plan to analyze the restrictions of our algorithm in learning networked LDS with spatially correlated inputs, and estimating directed networks with non-causal dependencies, where only approximate reconstruction may be possible using passive methods.

References

- [1] Riccardo Porreca, Samuel Drulhe, Hidde de Jong, and Giancarlo Ferrari-Trecate. Structural identification of piecewise-linear models of genetic regulatory networks. *Journal of Computational Biology*, 15(10):1365–1380, 2008.
- [2] Chushin Koh, Fang-Xiang Wu, Gopalan Selvaraj, and Anthony J Kusalik. Using a state-space model and location analysis to infer time-delayed regulatory networks. *EURASIP Journal on Bioinformatics and Systems Biology*, 2009:1–14, 2009.
- [3] James T Sandefur. *Discrete dynamical systems: Theory and applications*. Clarendon Press, 1990.
- [4] Julian Inchauspe, Ronald D Ripple, and Stefan Trück. The dynamics of returns on renewable energy companies: A state-space approach. *Energy Economics*, 48:325–335, 2015.

- [5] Anthony Stathopoulos and Matthew G Karlaftis. A multivariate state space approach for urban traffic flow modeling and prediction. *Transportation Research Part C: Emerging Technologies*, 11(2):121–135, 2003.
- [6] Fabrizio Ascione, Nicola Bianco, Rosa Francesca De Masi, Filippo de’Rossi, and Giuseppe Peter Vanoli. Simplified state space representation for evaluating thermal bridges in building: Modelling, application and validation of a methodology. *Applied Thermal Engineering*, 61(2):344–354, 2013.
- [7] Natalia Kroutikova, Carlos A Hernandez-Aramburo, and Timothy C Green. State-space model of grid-connected inverters under current control mode. *IET Electric Power Applications*, 1(3):329–338, 2007.
- [8] Arne Dankers, Paul MJ Van den Hof, Xavier Bombois, and Peter SC Heuberger. Errors-in-variables identification in dynamic networks—consistency results for an instrumental variable approach. *Automatica*, 62:39–50, 2015.
- [9] Donatello Materassi and Murti V Salapaka. On the problem of reconstructing an unknown topology via locality properties of the wiener filter. *IEEE transactions on automatic control*, 57(7):1765–1777, 2012.
- [10] Saurav Talukdar, Mangal Prakash, Donatello Materassi, and Murti V Salapaka. Reconstruction of networks of cyclostationary processes. In *2015 54th IEEE Conference on Decision and Control (CDC)*, pages 783–788. IEEE, 2015.
- [11] Saurav Talukdar, Deepjyoti Deka, Harish Doddi, Donatello Materassi, Michael Chertkov, and Murti V Salapaka. Physics informed topology learning in networks of linear dynamical systems. *Automatica*, 112:108705, 2020.
- [12] Sumanta Basu, George Michailidis, et al. Regularized estimation in sparse high-dimensional time series models. *The Annals of Statistics*, 43(4):1535–1567, 2015.
- [13] Po-Ling Loh, Martin J Wainwright, et al. High-dimensional regression with noisy and missing data: Provable guarantees with nonconvexity. *The Annals of Statistics*, 40(3):1637–1664, 2012.
- [14] Robert Tibshirani. Regression shrinkage and selection via the lasso. *Journal of the Royal Statistical Society: Series B (Methodological)*, 58(1):267–288, 1996.
- [15] Jerome Friedman, Trevor Hastie, and Robert Tibshirani. Sparse inverse covariance estimation with the graphical lasso. *Biostatistics*, 9(3):432–441, 2008.
- [16] Nicolai Meinshausen, Peter Bühlmann, et al. High-dimensional graphs and variable selection with the lasso. *Annals of statistics*, 34(3):1436–1462, 2006.
- [17] José Bento, Morteza Ibrahimi, and Andrea Montanari. Learning networks of stochastic differential equations. *arXiv preprint arXiv:1011.0415*, 2010.
- [18] Jitkomut Songsiri, Joachim Dahl, and Lieven Vandenbergh. Graphical models of autoregressive processes., 2010.
- [19] Max Simchowitz, Horia Mania, Stephen Tu, Michael I Jordan, and Benjamin Recht. Learning without mixing: Towards a sharp analysis of linear system identification. In *Conference On Learning Theory*, pages 439–473. PMLR, 2018.
- [20] Mohamad Kazem Shirani Faradonbeh, Ambuj Tewari, and George Michailidis. Finite time identification in unstable linear systems. *Automatica*, 96:342–353, 2018.
- [21] Salar Fattahi and Somayeh Sojoudi. Data-driven sparse system identification. In *2018 56th Annual Allerton Conference on Communication, Control, and Computing (Allerton)*, pages 462–469. IEEE, 2018.
- [22] Salar Fattahi, Nikolai Matni, and Somayeh Sojoudi. Learning sparse dynamical systems from a single sample trajectory. In *2019 IEEE 58th Conference on Decision and Control (CDC)*, pages 2682–2689. IEEE, 2019.
- [23] Christopher J Quinn, Negar Kiyavash, and Todd P Coleman. Directed information graphs. *IEEE Transactions on information theory*, 61(12):6887–6909, 2015.
- [24] Pradeep Ravikumar, Garvesh Raskutti, Martin J Wainwright, and Bin Yu. Model selection in gaussian graphical models: High-dimensional consistency of l1-regularized mle. In *NIPS*, pages 1329–1336, 2008.

- [25] Sahand N Negahban, Pradeep Ravikumar, Martin J Wainwright, Bin Yu, et al. A unified framework for high-dimensional analysis of m -estimators with decomposable regularizers. *Statistical science*, 27(4):538–557, 2012.
- [26] Pascal Massart. Some applications of concentration inequalities to statistics. In *Annales de la Faculté des sciences de Toulouse: Mathématiques*, volume 9, pages 245–303, 2000.
- [27] Michel Ledoux and Michel Talagrand. *Probability in Banach Spaces: isoperimetry and processes*. Springer Science & Business Media, 2013.
- [28] Sahand Negahban and Martin J Wainwright. Estimation of (near) low-rank matrices with noise and high-dimensional scaling. *The Annals of Statistics*, pages 1069–1097, 2011.
- [29] Michael Grant and Stephen Boyd. Cvx: Matlab software for disciplined convex programming, version 2.1, 2014.
- [30] Harish Doddi, Saurav Talukdar, Deepjyoti Deka, and Murti Salapaka. Exact topology learning in a network of cyclostationary processes. In *2019 American Control Conference (ACC)*, pages 4968–4973. IEEE, 2019.

7 Appendix

7.1 Proof of Lemma 3.1

Proof. From Eq. 10, we have $\frac{1}{U} \leq \lambda_{\min}[\Phi_x]$ and $\lambda_{\max}[\Phi_x] \leq \frac{1}{L}$. From Eqs. 4, 11, we have

$$\begin{aligned}
\|\Phi_x - \hat{\Phi}_x\|_2 &= \lim_{m \rightarrow \infty} \left\| \sum_{p=N}^m R_x(p) e^{-\iota f p} + \sum_{p=-m}^{-N} R_x(p) e^{-\iota f p} + \sum_{q=-(N-1)}^{N-1} \frac{|q|}{N} R_x(q) e^{-\iota f q} \right\|_2, \\
&\leq \lim_{m \rightarrow \infty} \left(\sum_{p=N}^m \|R_x(p)\|_2 + \sum_{p=-m}^{-N} \|R_x(p)\|_2 + \sum_{q=-(N-1)}^{N-1} \frac{|q|}{N} \|R_x(q)\|_2 \right), \\
&\leq \lim_{m \rightarrow \infty} \left(2 \sum_{p=N}^m C \delta^{-p} + 2 \sum_{q=1}^{N-1} C \frac{q}{N} \delta^{-q} \right) (\cdot \cdot \text{Eq. 10}) \\
&= 2C \delta^{-N} \frac{1}{1 - \delta^{-1}} + \frac{2C}{N} \left[\frac{\delta^{-1}(1 - \delta^{-N})}{(1 - \delta^{-1})^2} - \frac{N \delta^{-N}}{1 - \delta^{-1}} \right] \\
&= \frac{2C}{N} \left[\frac{\delta^{-1}(1 - \delta^{-N})}{(1 - \delta^{-1})^2} \right] \leq \frac{2C \delta^{-1}}{N(1 - \delta^{-1})^2}.
\end{aligned}$$

Therefore, if $N > \frac{4CU\delta^{-1}}{(1-\delta^{-1})^2}$, then $\|\Phi_x - \hat{\Phi}_x\|_2 \leq \frac{1}{2U}$. Moreover, for $v \in \mathbb{C}^{p+1}$ we have $\|(\hat{\Phi}_x)^{1/2} v\|_2^2 = v^H [\Phi_x - (\Phi_x - \hat{\Phi}_x)] v$. It thus follows that, $\|(\hat{\Phi}_x)^{1/2} v\|_2^2 \geq [\frac{1}{U} - \frac{1}{2U}] \|v\|_2^2 = \frac{1}{2U} \|v\|_2^2$, and $v^H \hat{\Phi}_x v \leq [\frac{1}{L} + \frac{1}{2U}] \|v\|_2^2$. Thus,

$$\frac{1}{2U} \|v\|_2^2 \leq v^H \hat{\Phi}_x v \leq \left[\frac{1}{L} + \frac{1}{2U} \right] \|v\|_2^2, \forall v \in \mathbb{C}^{p+1}. \quad (27)$$

Using the same approach,

$$\frac{1}{2U} \|v\|_2^2 \leq v^H \hat{\Phi}_{\bar{i}} v \leq \left[\frac{1}{L} + \frac{1}{2U} \right] \|v\|_2^2, \forall v \in \mathbb{C}^p.$$

□

7.2 M-estimator in complex-domain

Our estimator (Eq. 8) is a M-estimator in the complex domain. For completion, we present the proof of Eq. 14 and Proposition 1 by following the real-valued analysis in [25].

Eq. 14 states that if $\lambda \geq \frac{2}{n} \|\mathcal{X}^H(\mathcal{Y} - \mathcal{X}W_i)\|_\infty$ then $\hat{\Delta} := \hat{W}_i(\lambda) - W_i$ belongs to the set $\mathcal{D}(W_i) = \{\Delta \in \mathbb{C}^p \mid \|\Delta_{\mathcal{M}^\perp}\|_1 \leq 3\|\Delta_{\mathcal{M}}\|_1\}$.

To prove that, note that

$$\begin{aligned}
&\frac{1}{2n} [\|\mathcal{Y} - \mathcal{X}(W_i + \Delta)\|_2^2 - \|\mathcal{Y} - \mathcal{X}W_i\|_2^2] \\
&= \frac{1}{2n} [(\mathcal{Y}^H - (W_i + \Delta)^H \mathcal{X}^H)(\mathcal{Y} - \mathcal{X}(W_i + \Delta)) - (\mathcal{Y}^H - W_i^H \mathcal{X}^H)(\mathcal{Y} - \mathcal{X}W_i)] \\
&= \frac{1}{2n} [\Delta^H \mathcal{X}^H (\mathcal{X}W_i - \mathcal{Y}) + (\mathcal{X}W_i - \mathcal{Y})^H \mathcal{X} \Delta + \Delta^H \mathcal{X}^H \mathcal{X} \Delta] \\
&\geq \frac{1}{2n} 2 \operatorname{Re}(\langle \mathcal{X}^H (\mathcal{X}W_i - \mathcal{Y}), \Delta \rangle) \geq \frac{-1}{n} |\operatorname{Re}(\langle \mathcal{X}^H (\mathcal{X}W_i - \mathcal{Y}), \Delta \rangle)|,
\end{aligned}$$

where, $\operatorname{Re}(x)$ denotes the real part of the complex number x . Moreover,

$$\frac{1}{n} |\operatorname{Re}(\langle \mathcal{X}^H (\mathcal{X}W_i - \mathcal{Y}), \Delta \rangle)| \leq \frac{1}{n} |\langle \mathcal{X}^H (\mathcal{X}W_i - \mathcal{Y}), \Delta \rangle| \leq \frac{1}{n} \|\mathcal{X}^H (\mathcal{X}W_i - \mathcal{Y})\|_\infty \|\Delta\|_1 \leq \frac{\lambda}{2} \|\Delta\|_1.$$

Therefore, $\frac{1}{2n} [\|\mathcal{Y} - \mathcal{X}(W_i + \Delta)\|_2^2 - \|\mathcal{Y} - \mathcal{X}W_i\|_2^2] \geq -\frac{\lambda}{2} \|\Delta\|_1 = -\frac{\lambda}{2} (\|\Delta_{\mathcal{M}}\|_1 + \|\Delta_{\mathcal{M}^\perp}\|_1)$.

By optimality of $\hat{W}_i(\lambda) = W_i + \hat{\Delta}$ in the Regularized Wiener Filter Estimator,

$$\begin{aligned}
0 &\geq \frac{1}{2n} [\|\mathcal{Y} - \mathcal{X}(W_i + \hat{\Delta})\|_2^2 - \|\mathcal{Y} - \mathcal{X}W_i\|_2^2] + \lambda [\|W_i + \hat{\Delta}\|_1 - \|W_i\|_1] \\
&\geq -\frac{\lambda}{2} (\|\hat{\Delta}_{\mathcal{M}}\|_1 + \|\hat{\Delta}_{\mathcal{M}^\perp}\|_1) + \lambda (\|\hat{\Delta}_{\mathcal{M}^\perp}\|_1 - \|\hat{\Delta}_{\mathcal{M}}\|_1) = \frac{\lambda}{2} \|\hat{\Delta}_{\mathcal{M}^\perp}\|_1 - \frac{3\lambda}{2} \|\hat{\Delta}_{\mathcal{M}}\|_1.
\end{aligned}$$

Thus, $\hat{\Delta} \in \mathcal{D}(W_i)$. Next, we show that $\|\hat{W}_i - W_i\|_2 \leq (\frac{3}{\kappa}\lambda\sqrt{d})$, whenever Eq. 13 and Eq. 15 hold.

Proof of Proposition 1. Let $K(\delta) := \{\Delta \in \mathbb{C}^p \mid \Delta \in \mathcal{D}(W_i^f) \text{ and } \|\Delta\|_2 = \delta\}$. Let $F(\Delta)$ be the difference between the objective of the Regularized Wiener Filter Estimator evaluated at $W_i + \Delta$ and W_i . For a $\Delta \in K(\delta)$, the following holds:

$$\begin{aligned}
F(\Delta) &= \frac{1}{2n} [2\text{Re}\langle (\mathcal{X}^H(\mathcal{X}W_i - \mathcal{Y}), \Delta) + \Delta^H \mathcal{X}^H \mathcal{X} \Delta] + \lambda(\|W_i + \Delta\|_1 - \|W_i\|_1), \\
&\geq -\frac{1}{n} |\text{Re}\langle (\mathcal{X}^H(\mathcal{X}W_i - \mathcal{Y}), \Delta) | + \frac{\kappa}{2} \|\Delta\|_2^2 + \lambda(\|\Delta_{\mathcal{M}^\perp}\|_1 - \|\Delta_{\mathcal{M}}\|_1), \\
&\quad (\because \text{Using the restricted eigenvalue property}) \\
&\geq -\frac{\lambda}{2} \|\Delta\|_1 + \frac{\kappa}{2} \|\Delta\|_2^2 + \lambda(\|\Delta_{\mathcal{M}^\perp}\|_1 - \|\Delta_{\mathcal{M}}\|_1), \\
&\quad (\because \text{Using the condition on } \lambda) \\
&= \frac{\kappa}{2} \|\Delta\|_2^2 - \frac{3}{2} \lambda \|\Delta_{\mathcal{M}}\|_1 + \frac{1}{2} \lambda \|\Delta_{\mathcal{M}^\perp}\|_1, \\
&\geq \frac{\kappa}{2} \|\Delta\|_2^2 - \frac{3}{2} \lambda \|\Delta_{\mathcal{M}}\|_1, \\
&\geq \frac{\kappa}{2} \|\Delta\|_2^2 - \frac{3}{2} \lambda \sqrt{d} \|\Delta\|_2 \quad (\because \sup_{u \in \mathcal{M} \setminus \{0\}} \frac{\|u\|_1}{\|u\|_2} = \sqrt{d}), \\
&= (\frac{\kappa}{2} \|\Delta\|_2 - \frac{3}{2} \lambda \sqrt{d}) \|\Delta\|_2.
\end{aligned}$$

Thus, if $\|\Delta\|_2 = \delta > \frac{3}{\kappa} \lambda \sqrt{d}$, then, $F(\Delta) > 0$ for all $\Delta \in K(\delta)$. Note that $F(0) = 0$. Using Lemma 4 from the Supplementary material of [25] (uses convexity of $F(\Delta)$), it then follows that $\|\hat{\Delta}\|_2 \leq \delta$, that is, $\|\hat{W}_i - W_i\|_2 \leq (\frac{3}{\kappa} \lambda \sqrt{d})$. \square

7.3 Results on Covariance Matrices

Here we present few results on norms involving state covariance and error matrices that are used in the proofs in the main document.

Lemma 7.1. Suppose $Z := \mathcal{X}\Delta \in \mathbb{C}^n$ with non-i.i.d. rows in \mathcal{X} and Δ . The real component of Z is given by $Z_R = [\mathcal{X}_R - \mathcal{X}_I]v$ and the imaginary component is $Z_I = [\mathcal{X}_I \mathcal{X}_R]v$, for $v = [\Delta_R^T, \Delta_I^T]^T$. If $N > \frac{4CU\delta^{-1}}{(1-\delta^{-1})^2}$, then $\|\mathbb{E}[Z_R Z_R^T]\|_2 + \|\mathbb{E}[Z_I Z_I^T]\|_2 \leq 2\|\Delta\|_2^2 [\frac{1}{L} + \frac{1}{2U} + 4\sqrt{8}\frac{C}{\delta-1}]$.

Proof. For $r \in \{1, \dots, n\}$, X_i^r (r^{th} entry of \mathcal{Y}) and $(X_i^r)^T$ (r^{th} row of \mathcal{X}) are computed using N consecutive samples from $\{x((r-1)N), \dots, x((r-1)N + N - 1)\}$, using Eq. 5. For $r, c \in \{1, \dots, n\}$ we have,

$$\begin{aligned}
|\mathbb{E}[Z_R Z_R^T](r, c)| &= |v^T \mathbb{E} \begin{bmatrix} [\mathcal{X}_R(r, :)]^T \mathcal{X}_R(c, :) & -[\mathcal{X}_R(r, :)]^T \mathcal{X}_I(c, :) \\ -[\mathcal{X}_I(r, :)]^T \mathcal{X}_R(c, :) & [\mathcal{X}_I(r, :)]^T \mathcal{X}_I(c, :) \end{bmatrix} v|, \\
\Rightarrow |\mathbb{E}[Z_R Z_R^T](r, c)| &\leq \|\Delta\|_2^2 \mathbb{E} \begin{bmatrix} [\mathcal{X}_R(r, :)]^T \mathcal{X}_R(c, :) & -[\mathcal{X}_R(r, :)]^T \mathcal{X}_I(c, :) \\ -[\mathcal{X}_I(r, :)]^T \mathcal{X}_R(c, :) & [\mathcal{X}_I(r, :)]^T \mathcal{X}_I(c, :) \end{bmatrix} \Big\|_2. \quad (28)
\end{aligned}$$

$$\text{Similarly, } |\mathbb{E}[Z_I Z_I^T](r, c)| \leq \|\Delta\|_2^2 \mathbb{E} \begin{bmatrix} [\mathcal{X}_I(r, :)]^T \mathcal{X}_I(c, :) & [\mathcal{X}_I(r, :)]^T \mathcal{X}_R(c, :) \\ [\mathcal{X}_R(r, :)]^T \mathcal{X}_I(c, :) & [\mathcal{X}_R(r, :)]^T \mathcal{X}_R(c, :) \end{bmatrix} \Big\|_2. \quad (29)$$

Consider $\mathcal{Y}[1] = \frac{1}{\sqrt{N}} \sum_{t=0}^{N-1} x_i(t) e^{-\iota f t}$ and $\mathcal{Y}[2] = \frac{1}{\sqrt{N}} \sum_{s=0}^{N-1} x_i(s+N) e^{-\iota f s}$. The correlation between $\mathcal{Y}_R[1]$ and $\mathcal{Y}_R[2]$ is given by

$$\begin{aligned}
|\mathbb{E}[\mathcal{Y}_R[1] \mathcal{Y}_R[2]]| &= |\mathbb{E}[\frac{1}{N} \sum_{t=0}^{N-1} \sum_{s=0}^{N-1} x_i(t) x_i(s+N) \cos(ft) \cos(fs)]| \\
&= |\frac{1}{N} \sum_{t=0}^{N-1} \sum_{s=0}^{N-1} \mathbb{E}[x_i(t) x_i(s+N)] \cos(ft) \cos(fs)| \\
&\leq \frac{1}{N} \sum_{t=0}^{N-1} \sum_{s=0}^{N-1} |R_i(t-s-N)| = \frac{1}{N} \sum_{q=-(N-1)}^{N-1} (N-|q|) |R_i(q-N)|.
\end{aligned}$$

Expanding in time-domain (see Lemma 3.1's proof), it can be shown that

$$\|\mathbb{E}[\mathcal{X}_R(r, :)^T \mathcal{X}_R(c, :)]\|_2 \leq B^{rc}, \text{ where } B^{rc} := \frac{1}{N} \sum_{q=-(N-1)}^{N-1} (N - |q|) \|R_x(q + (r - c)N)\|_2. \quad (30)$$

Similarly, $\|\mathbb{E}[\mathcal{X}_R(r, :)^T \mathcal{X}_I(c, :)]\|_2$, $\|\mathbb{E}[\mathcal{X}_I(r, :)^T \mathcal{X}_I(c, :)]\|_2$, $\|\mathbb{E}[\mathcal{Y}_R[r] \mathcal{X}_I(c, :)]\|_2$, $\|\mathbb{E}[\mathcal{Y}_R[r] \mathcal{X}_R(c, :)]\|_2$, $\|\mathbb{E}[\mathcal{Y}_R[r] \mathcal{Y}_I[c]]\|_2$ and $\|\mathbb{E}[\mathcal{Y}_R[r] \mathcal{Y}_R[c]]\|_2$ are each upper bounded by B^{rc} . From Eqs. 28, 29, it follows that, $|\mathbb{E}[Z_R Z_R^T](r, c)| \leq \|\Delta\|_2^2 \sqrt{8} B^{rc}$ and $|\mathbb{E}[Z_I Z_I^T](r, c)| \leq \|\Delta\|_2^2 \sqrt{8} B^{rc}$. Thus,

$$\begin{aligned} \|\mathbb{E}[Z_R Z_R^T]\|_2 + \|\mathbb{E}[Z_I Z_I^T]\|_2 &\leq \max_{r=1}^n \sum_{c=1}^n |\mathbb{E}[Z_R Z_R^T](r, c)| + \max_{r=1}^n \sum_{c=1}^n |\mathbb{E}[Z_I Z_I^T](r, c)| \\ &\leq 2 \max_{r=1}^n \sum_{c=1}^n (|\mathbb{E}[Z_R Z_R^T](r, c)| + |\mathbb{E}[Z_I Z_I^T](r, c)|) \\ &= 2[v^T(\Sigma_1 + \Sigma_2)v + \max_r \sum_{c=1, c \neq r}^n (|\mathbb{E}[Z_R Z_R^T](r, c)| + |\mathbb{E}[Z_I Z_I^T](r, c)|)] \\ &\leq 2\|\Delta\|_2^2 \left[\left(\frac{1}{L} + \frac{1}{2U} \right) + \max_r \sum_{c, c \neq r} 2\sqrt{8} B^{rc} \right]. \end{aligned} \quad (31)$$

In the remaining, we find an upper bound for $\max_r \sum_{c, c \neq r} B^{rc}$. From Eq. 30,

$$\begin{aligned} B^{rc} &\leq \frac{1}{N} \sum_{q=-(N-1)}^{N-1} (N - |q|) C \delta^{-|q - cN + rN|}, \quad (\because \|R_x(\tau)\|_2 \leq C \delta^{-|\tau|}), \\ &= \frac{C}{N} \left[\sum_{q=1}^{N-1} (N - q) (\delta^{-| -q - cN + rN |} + \delta^{-| q - cN + rN |}) \right] + C \delta^{-| -cN + rN |}, \\ &= C \delta^{-|r - c|N} \left[\sum_{q=1}^{N-1} \left(1 - \frac{q}{N} \right) (\delta^q + \delta^{-q}) + 1 \right] \\ &= C \delta^{-|r - c|N} \left[1 + S_a + S_b - \frac{S_c}{N} - \frac{S_d}{N} \right], \end{aligned}$$

where, $S_a = \sum_{q=1}^{N-1} \delta^q = \frac{\delta^N - \delta}{\delta - 1}$, $S_c = \sum_{q=1}^{N-1} q \delta^q = \frac{\delta - \delta^N}{(\delta - 1)^2} + \frac{(N - 1)\delta^N}{\delta - 1}$,

$$S_b = \sum_{q=1}^{N-1} \delta^{-q} = \frac{1 - \delta^{-(N-1)}}{\delta - 1}, \quad S_d = \sum_{q=1}^{N-1} q \delta^{-q} = \frac{\delta^{-1} - \delta^{-N}}{(1 - \delta^{-1})^2} - \frac{(N - 1)\delta^{-N}}{1 - \delta^{-1}}.$$

$$\begin{aligned} \text{Thus, } \max_r \sum_{c=1, c \neq r}^n B^{rc} &\leq C \left[1 + S_a + S_b - \frac{S_c}{N} - \frac{S_d}{N} \right] \sum_{c=1, c \neq r}^n \delta^{-|r - c|N} \\ &\leq C \left[1 + S_a + S_b - \frac{S_c}{N} - \frac{S_d}{N} \right] \sum_{c=1}^{\infty} 2\delta^{-cN} \\ &\leq C \left[1 + S_a + S_b - \frac{S_c}{N} - \frac{S_d}{N} \right] \left[\frac{2\delta^{-N}}{1 - \delta^{-N}} \right], \\ &= C \left[1 + S_a + \frac{S_c}{N} (\delta^{-N} - 1) \right] \left[\frac{2\delta^{-N}}{1 - \delta^{-N}} \right] (\because \delta^N (S_b - \frac{S_d}{N}) = \frac{S_c}{N}), \\ &\leq C(1 + S_a) \frac{2\delta^{-N}}{1 - \delta^{-N}} (\because \delta^{-N} - 1 \text{ is negative and can be ignored}), \\ &\leq C(1 + \frac{\delta^N - \delta}{\delta - 1}) \frac{2\delta^{-N}}{1 - \delta^{-N}} = C \left(\frac{\delta^N - 1}{\delta - 1} \right) \left(\frac{2}{\delta^N - 1} \right) = \frac{2C}{\delta - 1}. \end{aligned} \quad (32)$$

Substituting Eq. 32 in Eq. 31 gives $\|\mathbb{E}[Z_R Z_R^T]\|_2 + \|\mathbb{E}[Z_I Z_I^T]\|_2 \leq 2\|\Delta\|_2^2 \left[\frac{1}{L} + \frac{1}{2U} + 4\sqrt{8} \frac{C}{\delta - 1} \right]$. \square

Lemma 7.2 (covariance (restart & record)). *Let $\mathcal{E} := \mathcal{Y} - \mathcal{X}W_i$ with each row corresponding to an i.i.d. trajectory. Let $\mathcal{E}_1 := [\mathcal{E}_R[1] \ \mathcal{E}_I[1] \ \dots \ \mathcal{E}_R[n] \ \mathcal{E}_I[n]]^T$ be the re-arranged vector of real and complex entries in \mathcal{E} , with covariance matrix $\mathcal{C}_1 = \mathbb{E}[\mathcal{E}_1 \mathcal{E}_1^T]$. Then $\|\mathcal{C}_1\|_2 \leq \frac{3}{2L}$.*

Proof. As the n trajectories are i.i.d.,

$$\mathcal{C}_1 := \text{diag}(\mathbf{C}, \dots, \mathbf{C}), \text{ where } \begin{pmatrix} \mathcal{E}_R(j) \\ \mathcal{E}_I(j) \end{pmatrix} \sim \mathcal{N}(\mathbf{0}, \mathbf{C}) \Rightarrow \|\mathcal{C}_1\|_2 = \|\mathbf{C}\|_2. \quad (33)$$

Consider $\mathbf{E} = \Phi_i - \Phi_{i,\bar{i}} W_i - (W_i)^H \Phi_{\bar{i},i} + (W_i)^H \Phi_{\bar{i}} W_i$. Substituting $W_i = [\Phi_{\bar{i}}]^{-1} \Phi_{i,\bar{i}}$ in \mathbf{E} and using the Schur complement lemma, we get,

$$\mathbf{E} = \Phi_i - \Phi_{i,\bar{i}} (\Phi_{\bar{i}})^{-1} \Phi_{\bar{i},i} = \frac{1}{[\Phi_x]^{-1}(i, i)}. \quad (34)$$

From the definition of L , U in Eq. 10, we have, $\frac{1}{U} \leq \mathbf{E} \leq \frac{1}{L}$ and $(1 + \|W_i\|_2^2) \frac{1}{U} \leq \mathbf{E} \leq (1 + \|W_i\|_2^2) \frac{1}{L}$. Comparing the two bounds, we get

$$\frac{L}{U} \leq (1 + \|W_i\|_2^2) \leq \frac{U}{L}. \quad (35)$$

From the definition of \mathcal{E} , it follows that $\mathbb{E}[\mathcal{E}[j]^H \mathcal{E}[j]] = \hat{\Phi}_i - \hat{\Phi}_{i,\bar{i}} W_i - (W_i)^H \hat{\Phi}_{\bar{i},i} + (W_i)^H \hat{\Phi}_{\bar{i}} W_i$. Define $V = \hat{\Phi}_x - \Phi_x$, and from Lemma 3.1, we have $\|V\|_2 \leq \frac{1}{2U}$. Substituting $\hat{\Phi}_x = \Phi_x + V$ in $\mathbb{E}[\mathcal{E}[j]^H \mathcal{E}[j]]$, we get,

$$\begin{aligned} \mathbb{E}[\mathcal{E}[j]^H \mathcal{E}[j]] &= \frac{1}{[\Phi_x]^{-1}(1, 1)} + V_i - V_{i,\bar{i}} W_i - (W_i)^H V_{\bar{i},i} + (W_i)^H V_{\bar{i}} W_i \quad (\because \text{ using Eq. 34}), \\ \Rightarrow \mathbb{E}(\mathcal{E}_R[j]^2) + \mathbb{E}(\mathcal{E}_I[j]^2) &= \text{Tr}(\mathbf{C}) \leq \frac{1}{L} + (1 + \|W_i\|_2^2) \|V\|_2 \leq \frac{1}{L} + \frac{U}{L} \frac{1}{2U} = \frac{3}{2L} \quad (\because \text{ using Eq. 35}) \\ \Rightarrow \|\mathcal{C}_1\|_2 = \|\mathbf{C}\|_2 &\leq \frac{3}{2L}. \end{aligned} \quad (36)$$

□

Lemma 7.3 (covariance (consecutive)). *Let $\mathcal{E} := \mathcal{Y} - \mathcal{X} W_i$ with non-i.i.d. trajectories per row. Let $\mathcal{E}_1 := [\mathcal{E}_R[1] \ \mathcal{E}_I[1] \ \dots \ \mathcal{E}_R[n] \ \mathcal{E}_I[n]]^T$ be the re-arranged vector of real and complex entries in \mathcal{E} with covariance matrix $\mathbf{C}_1 = \mathbb{E}[\mathcal{E}_1 \mathcal{E}_1^T]$. Then $\|\mathbf{C}_1\|_2 \leq \frac{3}{2L} + 54 \frac{U}{L} \frac{2C}{\delta-1}$.*

Proof. Writing real and imaginary parts of \mathcal{E}_1 and using inequality of matrix 2 and ∞ -norms, we have,

$$\begin{aligned} \|\mathbf{C}_1\|_2 &\leq \max \left[\max_{r=1}^n \sum_{c=1}^n \left(|\mathbb{E}[\mathcal{E}_R \mathcal{E}_R^T](r, c)| + |\mathbb{E}[\mathcal{E}_R \mathcal{E}_I^T](r, c)| \right), \max_{r=1}^n \sum_{c=1}^n \left(|\mathbb{E}[\mathcal{E}_I \mathcal{E}_R^T](r, c)| + |\mathbb{E}[\mathcal{E}_I \mathcal{E}_I^T](r, c)| \right) \right], \\ &\leq \max \left[\max_{r=1}^n \sum_{c=1, c \neq r}^n \left(|\mathbb{E}[\mathcal{E}_R \mathcal{E}_R^T](r, c)| + |\mathbb{E}[\mathcal{E}_R \mathcal{E}_I^T](r, c)| \right), \max_{r=1}^n \sum_{c=1, c \neq r}^n \left(|\mathbb{E}[\mathcal{E}_I \mathcal{E}_R^T](r, c)| + |\mathbb{E}[\mathcal{E}_I \mathcal{E}_I^T](r, c)| \right) \right] + \frac{3}{2L} \quad (\because \text{ Using Eq. 36}). \end{aligned} \quad (37)$$

Split $\mathcal{E} = \mathcal{Y} - \mathcal{X} W_i$ into their real and imaginary parts (subscripted by R and I respectively). Now $\mathcal{E}_R = [\mathcal{Y}_R \ -\mathcal{X}_R \ \mathcal{X}_I] [1 \ (W_i)_R \ (W_i)_I]^T$, and $\mathcal{E}_I = [\mathcal{Y}_I \ -\mathcal{X}_I \ -\mathcal{X}_R] [1 \ (W_i)_R \ (W_i)_I]^T$. For $r, c \in \{1, \dots, n\}$, $r \neq c$, the correlation between the r^{th} and c^{th} sample is

$$\mathbb{E}[\mathcal{E}_R[r] \mathcal{E}_R[c]] = \begin{bmatrix} 1 & (W_i)_R & (W_i)_I \end{bmatrix} \begin{bmatrix} \mathbb{E}(\mathcal{Y}_R[r] \mathcal{Y}_R[c]) & -\mathbb{E}(\mathcal{Y}_R[r] \mathcal{X}_R(c, :)) & \mathbb{E}(\mathcal{Y}_R[r] \mathcal{X}_I(c, :)) \\ -\mathbb{E}(\mathcal{X}_R(r, :)^T \mathcal{Y}_R[c]) & \mathbb{E}(\mathcal{X}_R(r, :)^T \mathcal{X}_R(c, :)) & -\mathbb{E}(\mathcal{X}_R(r, :)^T \mathcal{X}_I(c, :)) \\ \mathbb{E}(\mathcal{X}_I(r, :)^T \mathcal{Y}_R[c]) & -\mathbb{E}(\mathcal{X}_I(r, :)^T \mathcal{X}_R(c, :)) & \mathbb{E}(\mathcal{X}_I(r, :)^T \mathcal{X}_I(c, :)) \end{bmatrix} \begin{bmatrix} 1 \\ (W_i)_R \\ (W_i)_I \end{bmatrix}.$$

From Eq. 30 and Eq. 35, it follows that, $|\mathbb{E}[\mathcal{E}_R[r] \mathcal{E}_R[c]]| \leq \frac{U}{L} \sqrt{27} B^{rc}$. Similarly,

$$|\mathbb{E}[\mathcal{E}_R[r] \mathcal{E}_I[c]]| \leq \frac{U}{L} \sqrt{27} B^{rc}, |\mathbb{E}[\mathcal{E}_I[r] \mathcal{E}_R[c]]| \leq \frac{U}{L} \sqrt{27} B^{rc}, |\mathbb{E}[\mathcal{E}_I[r] \mathcal{E}_I[c]]| \leq \frac{U}{L} \sqrt{27} B^{rc}. \quad (38)$$

Using the inequalities Eq. 38 in Eq. 37, we have $\|\mathbf{C}_1\|_2 \leq \frac{3}{2L} + 2\sqrt{27} \sum_{c=1, c \neq r}^n \frac{U}{L} B^{rc}$. Then, it follows from Eq. 32,

$$\|\mathbf{C}_1\|_2 \leq \frac{3}{2L} + 6\sqrt{3} \frac{U}{L} \frac{2C}{\delta-1}. \quad (39)$$

□